Journal of Natural Fibers

ISSN: 1544-0478 (Print) 1544-046X (Online) Journal homepage: www.tandfonline.com/journals/wjnf20

An Experimental Study on Low-Velocity Impact Behavior of Carbon Fiber/Pineapple Leaf Fiber Hybrid Laminates for Automotive Applications

Hanyue Xiao, Mohamed Thariq Hameed Sultan, Farah Syazwani Shahar & Suhas Yeshwant Nayak

To cite this article: Hanyue Xiao, Mohamed Thariq Hameed Sultan, Farah Syazwani Shahar & Suhas Yeshwant Nayak (2025) An Experimental Study on Low-Velocity Impact Behavior of Carbon Fiber/Pineapple Leaf Fiber Hybrid Laminates for Automotive Applications, Journal of Natural Fibers, 22:1, 2448015, DOI: 10.1080/15440478.2024.2448015

To link to this article: https://doi.org/10.1080/15440478.2024.2448015

JOURNAL OF NATURAL FIBERS
2025, VOL. 22, NO. 1, 2448015
https://doi.org/10.1080/15440478.2024.2448015

An Experimental Study on Low-Velocity Impact Behavior of Carbon Fiber/Pineapple Leaf Fiber Hybrid Laminates for Automotive Applications

Hanyue Xiao[a,b], Mohamed Thariq Hameed Sultan[a,c,d], Farah Syazwani Shahar[a], and Suhas Yeshwant Nayak[e]

[a]Department of Aerospace Engineering, Faculty of Engineering, Universiti Putra Malaysia, Serdang, Selangor Darul Ehsan, Malaysia; [b]School of Intelligent Manufacturing and Automobile, Chongqing College of Electronic Engineering, Chong Qing, China; [c]Laboratory of Biocomposite Technology, Institute of Tropical Forestry and Forest Products (INTROP), Universiti Putra Malaysia, Serdang, Selangor Darul Ehsan, Malaysia; [d]Aerospace Malaysia Innovation Centre (944751-A), Prime Minister's Department, MIGHT Partnership Hub, Cyberjaya, Selangor Darul Ehsan, Malaysia; [e]Department of Mechanical and Industrial Engineering, Manipal Institute of Technology, Manipal Academy of Higher Education, Manipal, Karnataka, India

ABSTRACT
This work characterizes the low-velocity impact (LVI) failure behaviors of three bio/synthetic hybrid laminates based on carbon fiber (C) and pineapple leaf fiber (P). The effect of aluminum (A) addition and its position were investigated by flexural tests, peak force, force–displacement curves, energy–time curves, visual inspection, and infrared thermography (IR). The flexural tests reveal that fiber-reinforced polymer (FRP) CPC composites exhibit superior flexural properties than fiber metal laminates (FMLs). FMLs with aluminum as skin sheets (ACPCA) show a 62.2% improvement in flexural strength (312.02 MPa) over those with internal aluminum (CAPAC). LVI results show that FMLs outperform FRP in impact performance, with ACPCA and CAPAC achieving peak force improvements of 266.22% (2.71 kN) and 209.50% (2.29 kN) over CPC (0.74 kN), respectively. The results emphasize the significance of A position, where ACPCA exhibits full rebound behavior while CAPAC shows partially rebound at 15J impact energy. Visual inspection and IR results corroborate LVI findings, indicating increased delamination at higher energies. Notably, IR provides critical insights into damage progression and internal structural changes, highlighting areas of delamination and deformation around V-type damage. These results suggest that the ACPAC provides a balance between bending and impact resistance, assisting material selection in automotive applications.

摘要
这项工作表征了基于碳纤维（C）和菠萝叶纤维（P）的三种生物/合成杂化层压板的低速冲击（LVI）破坏行为． 通过弯曲试验、峰值力、力-位移曲线、能量-时间曲线、目视检查和红外热成像（IR）研究了铝（A）添加及其位置的影响. 弯曲试验表明，纤维增强聚合物（FRP）CPC复合材料的弯曲性能优于纤维金属层压板（FML）. 使用铝作为蒙皮的FML（ACPCA）的抗弯强度（312.02 MPa）比使用内部铝（CAPAC）的FML提高了62.2%. LVI结果表明，FML在冲击性能方面优于FRP，ACPCA和CAPAC的峰值力分别比CPC（0.74 kN）提高了266.22%（2.71 kN）和209.50%（2.29 kN）. 结果强调了A

KEYWORDS
Fiber metal laminates; pineapple leaf fiber; carbon fiber; low-velocity impact; non-destructive testing

关键词
纤维金属层压板; 菠萝叶纤维; 碳纤维; 低速冲击; 无损检测

CONTACT Mohamed Thariq Hameed Sultan thariq@upm.edu.my Department of Aerospace Engineering, Faculty of Engineering, Universiti Putra Malaysia, Serdang, Selangor Darul Ehsan 43400 UPM, Malaysia; Suhas Yeshwant Nayak suhas.nayak@manipal.edu Department of Mechanical and Industrial Engineering, Manipal Institute of Technology, Manipal Academy of Higher Education, Manipal, Karnataka 576104, India

位置的重要性，其中ACPCA表现出完全回弹行为，而CAPAC在15J冲击能量下表现出部分回弹. 目视检查和IR结果证实了LVI的发现，表明在较高能量下分层增加. 值得注意的是，IR提供了对损伤进展和内部结构变化的关键见解，突出了V型损伤周围的分层和变形区域. 这些结果表明，ACPAC在抗弯曲性和抗冲击性之间实现了平衡，有助于汽车应用中的材料选择.

Introduction

In the face of fierce market competition and consistent enhancement of consumer demands in the automotive market, research and development for new automotive materials have accelerated. FMLs typically consist of thin layers of metal interleaved with layers of high-strength fibers, such as aramid fiber, glass fiber (G), carbon fibers (C), kevlar fiber (K), bonded together with a matrix material (Askarian Khoob, Ramezani, and Mousavi 2023; Hussain et al. 2022; Khalid et al. 2021; Muflikhun and Yokozeki 2021). Compared with other traditional materials in the automotive industry, FMLs exhibit superior impact performance due to their unique combination of metal and FRP composite layers (Pang et al. 2022). Combining metal and FRP composite allows FMLs to absorb and dissipate impact energy more effectively than traditional materials. The metal layers provide ductility and toughness, while the fiber-reinforced layers contribute strength and stiffness. In addition, FMLs offer a high strength-to-weight ratio, making them lightweight while maintaining structural integrity. This is particularly advantageous in applications where minimizing weight is crucial for fuel efficiency and overall vehicle performance. Thus, FMLs find utility in components such as bumpers, body panels, door reinforcements, and interior structures, enhancing impact absorption, reducing the risk of damage in low-speed collisions, and improving crashworthiness while simultaneously reducing overall vehicle weight, contributing to improved safety and fuel efficiency (Allah et al. 2023; Pang et al. 2022; Xiao, Sultan, Shahar, Gaff, et al. 2023; Zhang and Xu 2022). Despite considerations such as cost and manufacturing complexity, the remarkable impact performance of FMLs positions them as compelling materials for advancing safety and efficiency in automotive applications.

Additionally, recent studies have highlighted the importance of natural fiber-reinforced polymer (NFRP) composites in advancing the sustainability of FMLs. By using renewable and biodegradable natural fibers, NFRP composites decrease dependence on petrochemical materials, lower the carbon footprint, and offer better end-of-life solutions through enhanced recyclability and biodegradability (Ilyas et al. 2022; Sari et al. 2023; Syafri et al. 2023). Various natural fibers such as sisal fiber (Vieira et al. 2022), jute fiber (Abd El-Baky et al. 2022; Allah et al. 2023), bamboo fiber (Kali, Pathak, and Korla 2020), hemp fiber (R et al. 2020), and P (Ng et al. 2023) are increasingly utilized in FMLs to produce lighter and more durable automotive components, which enhances fuel efficiency and reduces carbon emissions (Babu et al. 2021; Dua et al. 2023). Despite these benefits, challenges such as moisture absorption, variable mechanical properties, and limited high-performance applications must be addressed (Herlina Sari et al. 2024). To overcome these issues, recent research has focused on developing hybrid bio/synthetic FMLs that balance mechanical performance with environmental sustainability. Giammaria et al. (2023) researched bio-composite laminates reinforced by flax, basalt, and hybrid fibers, focusing on LVI testing. Their study revealed that the impact resistance from combining flax fibers with basalt fibers was less temperature-dependent than pure flax laminates. Baigh et al. (2023) also found that hybrid jute/P biocomposites significantly outperformed the P-reinforced composites in terms of tensile, flexural, and impact strength. Feng et al. (2022) Ng et al. (2023) observed the impact resistance of hybrid A/G/P laminates by the Charpy impact test. Their results indicated that the hybrid FMLs have intermedium impact strength between non-hybrid FMLs with fully synthetic and natural fibers. In addition, they concluded that the outermost layers in hybrid core composites play a vital role in impact performance. Murugu Nachippan et al. (2021) demonstrated that hybrid G/hemp fiber coreinforced polymer exhibited superior impact strength compared to single G-reinforced composites. Overall, hybrid FMLs balance impact performance, cost, and sustainable development. It can mitigate the negative impact on drivers in the event of a collision, making it suitable for applications in car bodies and bumpers.

For these newly emerging materials, such as hybrid bio/synthetic FMLs in the automotive industry, impact tests are crucial in evaluating the safety and performance of materials used in vehicle construction (Fragoso-Medina and Velázquez-Villegas 2023; Ganesarajan et al. 2022). These tests simulate real-world collision scenarios, providing valuable insights into a material's ability to withstand various energy forces. By assessing crashworthiness, impact tests contribute to the optimization of vehicle design, aiding in selecting materials that enhance occupant safety (Mohammadi et al. 2022; Noorsumar et al. 2022). Moreover, they ensure compliance with rigorous safety standards and regulations, fostering consumer confidence and enabling manufacturers to create vehicles that meet and often exceed industry safety benchmarks (Zhang and Xu 2022). Different types of impact tests such as Charpy, Izod, low-velocity impact (LVI), and high-velocity impact tests (HVI), are commonly utilized to evaluate the impact behavior of materials, providing distinct insights into their performance under various conditions (Doddamani et al. 2023; Miao et al. 2022; Ravi et al. 2022). The selection of an impact test depends on the specific requirements and material application, considering factors such as cost, simplicity, and the level of detail needed in impact analysis. Among these test, LVI tests incorporate advanced instrumentation to record force–time or displacement–time curves, offering more comprehensive insights into a material's response to impact loading (Abid et al. 2022; Ravi et al. 2022). Engineers use the data generated from low-velocity impact testing to optimize material designs for durability and reliability in real-world usage conditions, ensuring structures can withstand common impact events (Stephen et al. 2021).

Understanding the failure mechanisms of materials after impact tests is critical for optimizing material design and performance. LVI tests can cause different types of damage, including delamination, fiber breakage, and matrix cracking (Siddiqui, Rabbi, and Dewanjee 2023). According to Pang et al. (2022), delamination between fiber and metal is the dominant failure mode under the low-energy impact. In contrast, higher-energy impacts result in dominant metal and FRP fractures. However, the damage mechanisms of FMLs are more complex compared to non-hybrid materials due to the layered structure composed of different materials with distinct mechanical properties, and the interactions between layers give rise to intricate failure modes. Thus, compared with other inspection methods, nondestructive testing (NDT) is particularly valuable for evaluating damage to FMLs after impact testing without causing further damage (Najeeb et al. 2021). In recent years, various NDT techniques, such as ultrasonic testing (Barth et al. 2023), eddy current testing (Xie et al. 2023), X-ray tomography (Shah et al. 2023), thermography (Bornemann and Lang 2022; Liu et al. 2023), etc., have been employed to assess the internal and surface conditions of FMLs materials. These NDT methods are essential for gaining insights into material conditions after impact testing, enabling precise analysis to ensure the reliability and safety of materials without compromising their structural integrity.

In Malaysia, there is significant agricultural waste from pineapple leaves, with pineapple leaf fiber being notable for its low density, degradability, and excellent mechanical properties (Chrispin Das et al. 2022; Feng et al. 2022). Researchers have thus explored pineapple leaf fiber as reinforcements in eco-friendly composites with improved mechanical performance and sustainability, but its application in automotive materials remains limited and under-researched (Jain, Jain, and Sinha 2018; Siakeng et al. 2019). Thus, this study aims to address this gap by exploring the use of pineapple leaf waste in hybrid laminates and evaluating their effectiveness for automotive applications. This research specifically focuses on a novel combination of A sheet, high-strength C, and eco-friendly P, a combination that has not been previously investigated. The flexural test, LVI test, visual inspection, and NDT test were carried out to investigate the mechanical properties and LVI behavior of hybrid FRP composites and FMLs. Additionally, the effect of A layers and layer sequence were also researched in three variations. Through this research, we seek to advance the development of sustainable materials which balance mechanical performance with eco-friendliness for automotive practical applications (Aili Hamzah et al. 2021).

Methodology

Materials

All the reinforcements were provided by Mechasolve Engineering Sendirian Berhad (MESB), Malaysia. The woven P fabric utilized in the experiments has a thickness of 0.78 mm and an areal density of 315 g/m^2. A 12 K unidirectional C Fabric with a thickness of 0.28 mm and an areal density of 210 g/m^2. Aluminum 6061–T6 sheets have a density of 2.7 g/cm^3 and a thickness of 0.4 mm. To improve the resin infusion process, water jet cutting was used to drill 1 mm diameter holes at a spacing of 75 mm on the bare aluminum sheets to manufacture FMLs composites (Ortiz de Mendibil et al. 2016). In order to create a rougher surface finish and increase the interfacial bonding between A layers and the matrix, the A sheets underwent mechanical polishing, followed by alkaline etching and sulfuric acid anodizing (Hynes et al. 2022; Wu et al. 2020; Zhu et al. 2019). In addition, thermoset composite epoxy was chosen in the present study due to its outstanding performance, including lightweight, excellent chemical resistance, and satisfactory mechanical performance (Xiao, Sultan, Shahar, Gaff, et al. 2023). The epoxy EpoxAmiteTM 100 and the hardener EpoxAmiteTM 103 were provided by Smooth-On company.

Layering sequence

The configuration of the stacking sequence is crucial in determining the mechanical characteristics of C/P laminates (Hashim et al. 2023). Based on our previous study, a 2:1 ratio of C to P significantly outperforms a 1:2 ratio in terms of mechanical properties. Specifically, FMLs with the 2:1 C to P ratio showed a 65.5% increase in tensile strength and a 57.3% increase in flexural strength compared to those with the 1:2 ratio (Xiao, Sultan, Shahar, Nayak, et al. 2023). Additionally, these FMLs exhibited a 26.3% improvement in interlaminar shear strength (ILSS) and a 38.4% enhancement in Izod impact strength over the 1:2 ratio (Xiao et al. 2024). Therefore, the 2:1 CF to PALF ratio was chosen for its superior mechanical performance in our research. The sample stacking sequence is shown in Figure 1. Hybrid FRP composite CPC adopts a sandwich structure consisting of two layers of C as the outer layer and one layer of P as the core layer. Two hybrid FMLs have a symmetrical structure composed of five layers. The FMLs ACPCA was created by wrapping the CPC with a layer of A plate on both sides.

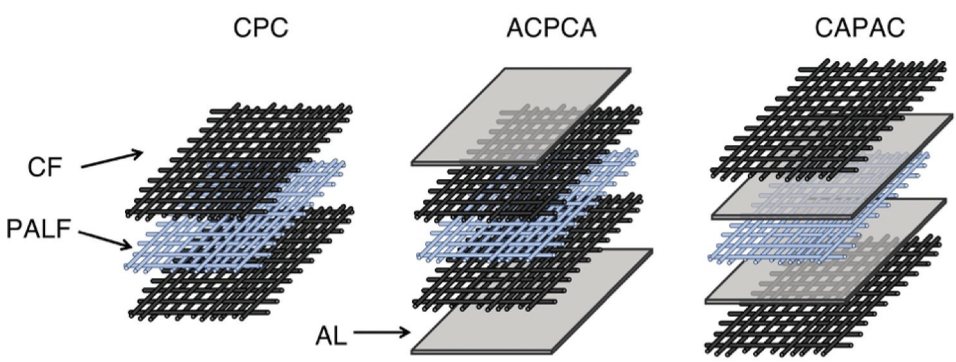

Figure 1. Schematic illustration of three hybrid laminates.

The FMLs CAPAC changed the position of carbon fiber and aluminum sheets; thus, the effect of the layering sequence on impact performance could be observed.

Manufacturing process

The hybrid laminates were fabricated with 300 × 300 mm dimensions by the vacuum-assisted resin transfer molding (VARTM) method. Compared with hand lay-up, VARTM is offers several advantages including provide good interfacial bonding, more uniform resin distribution, high fiber volume fraction, and the ability to produce larger and more complex parts (Xiao, Sultan, Shahar, Gaff, et al. 2023). Figure 2 depicts the schematic illustration of the significant components of the VARTM setup: a vacuum pump, a mold, sealant tape, a peel ply, an infusion mesh, a vacuum bag, a resin container, and an intake and outlet tube. The glass mold was first cleaned with acetone to remove dust or impurities. Next, a layer of wax was applied, allowed to solidify for ten minutes, and then wiped off. These steps were carried out three times to create a good wax layer that could be easily removed. Following that, all the piles were put on the mold in the design order, as Figure 2 shows. Lastly, a VARTM-sealed environment is created by taping a flexible vacuum bag to the mold. The resin infusion process began with a 100:28.4 weight ratio mixture of epoxy and hardener. When the resin is ready, it is immediately transported into the storage tank and linked to the inlet tube for resin infusion. The composite curing procedure takes at least 24 hours at room temperature. The experimental setup of the VARTM process is shown in Figure 3. Key challenges during VARTM process include ensuring complete and uniform resin flow, and preventing void formation, which can compromise mechanical properties. Despite the more complex and time-consuming setup, VARTM still is a preferred choice for fabricating high-quality laminated composites.

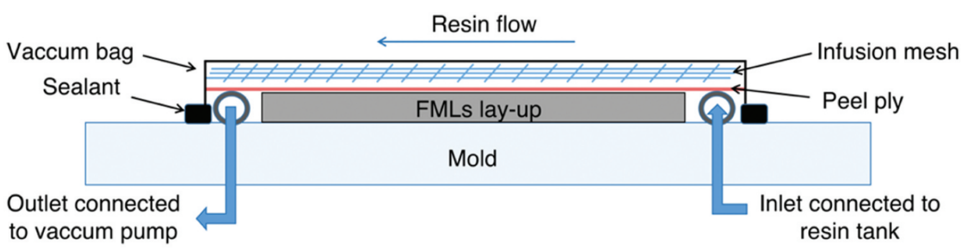

Figure 2. Schematic illustration of the VARTM process.

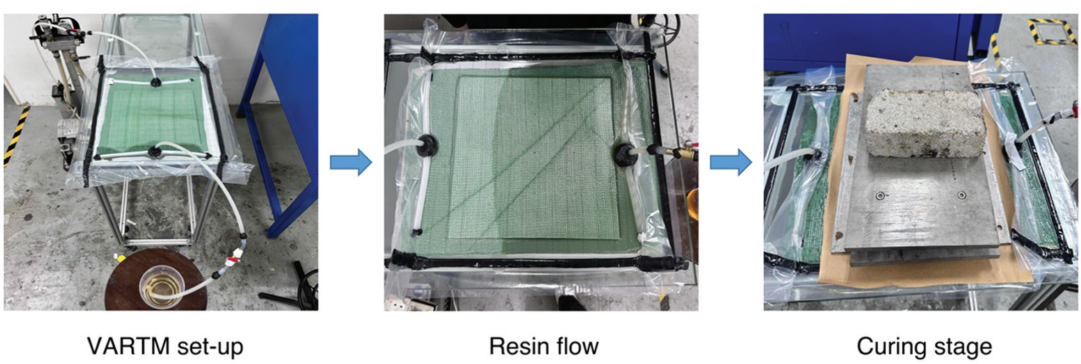

Figure 3. Experimental setup of VARTM.

Physical properties characterization

The physical properties including the thicknesses and weight of the fabricated samples were recorded by calipers and digital precision balance, respectively. The fiber weight fraction and metal volume fraction (MVF) was calculated by Equation 1 and Equation 2 (Kosedag, Aydin, and Ekici 2022), respectively.

$$\text{Fiber weight fraction} = \frac{w_{fiber}}{w_{composites}} \tag{1}$$

w_{fiber} = the total fiber weight,
$w_{composites}$ = the total composites weight.

$$\text{MVF} = \frac{\sum_{1}^{n} t_{metal}}{t_{composites}} \tag{2}$$

n = the number of metal layers,
t_{metal} = the thickness of each metal sheet,
$t_{composites}$ = the total thickness of the composites.

Flexural test

The flexural test was conducted using INSTRON 5567 at the Institute of Tropical Forestry and Forest Products, Universiti Putra Malaysia, Malaysia. The three-point bending test's sample dimension was 127 mm × 12.7 mm according to the ASTM D790 standard (Gupta, Mahato, and Bhattacharya 2022). In the flexural test, the quasi-static cross-head speed was maintained at 2 mm/min, and the span-to-thickness ratio was 16:1. Every variation was tested using five replications, and an average value was recorded.

LVI test

The LVI test setup is shown in Figure 4. The impact tests were conducted using the Imatek IM10 drop weight impact tester at the Department of Aerospace Engineering, Universiti Putra Malaysia. The striker with a hemispherical tip diameter of 16 mm and a weight of 5.101 kg was positioned so as to be perpendicular to the center of the FMLs plate plane, thus creating concentrated throughout-of-plane impact damage. Four clamps (Figure 4b) were employed to secure the specimen during the impact, and their placement could impact the magnitude of the contact force and the overall duration of the impact (Vieira et al. 2022). The LVI test is carried out according to ASTM D7136 (Najeeb et al. 2021). The testing temperature was maintained at a standard room temperature of approximately 65 degrees Fahrenheit, and the relative humidity level was kept at around 60%. The samples' dimensions were 100 mm × 150 mm (Figure 4c). Throughout the tests, the impactor consistently rebounded after the impact and was captured by the pneumatic brake to prevent any unintended additional strikes. The impact energy (E) was calculated using the Equation (3). Pilot experiments were conducted on all laminates using varying impact energies to ensure the reliability of our research.

$$E = mgh \tag{3}$$

m = mass of the striker (kg),
g = the gravitational acceleration (ms^{-2}),
h =the height of the impactor (m).

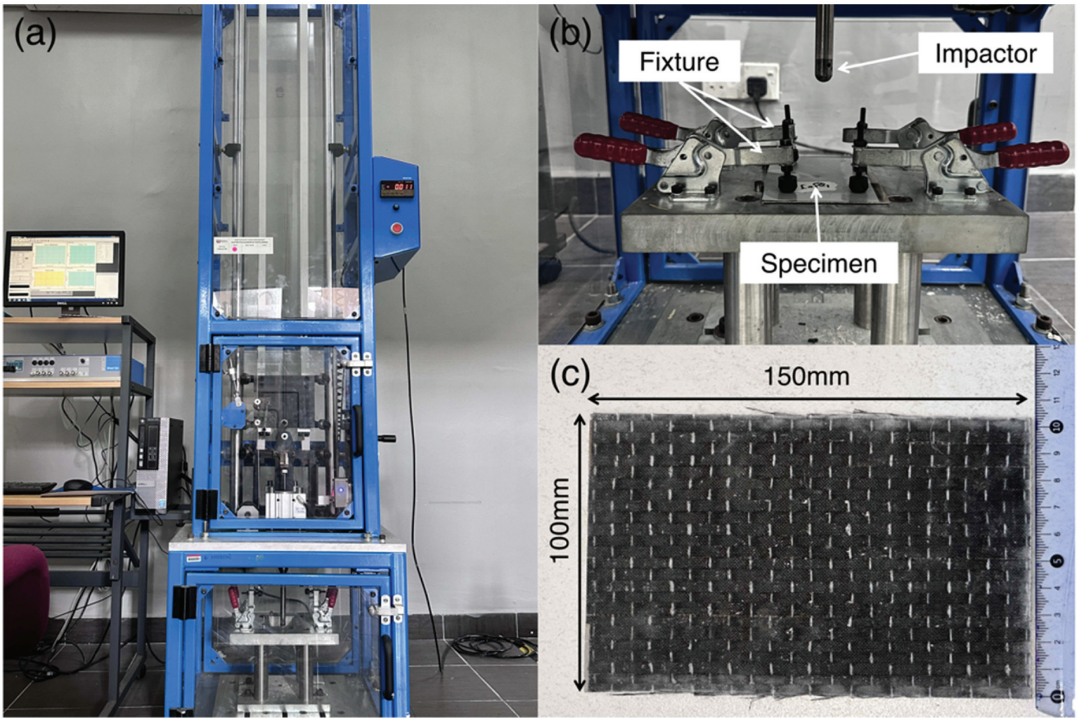

Figure 4. LVI tests setup: (a) overview of the drop tower machine, (b) enlargement of the fixtures for the samples, (c) dimension of the specimens for LVI tests.

Infrared thermography test

The subsurface features of low-velocity impacted specimens were evaluated using the IR technique. The advantages of the IR technique include its ability to quickly and safely scan large areas without causing damage, saving time, and posing no potential hazards because it emits no radiation (Zhu et al. 2022). The setup of the IR test is shown in Figure 5. The heat lamps with a maximum power of 500W were used as external stimulus sources to provide appropriate thermal contrasts. The infrared camera OPTRIS PI 640i (Germany) was utilized to monitor the temperature differences on the investigated surface. This camera boasts a thermal sensitivity of 40 mK, operates at a frame rate of 32 hz and a resolution of 640 × 480 pixels. The distance between the heat lamps and the specimen was 40 cm, and the distance between the infrared camera and the specimen was fixed at 100 cm. The ambient temperature was controlled and maintained at around 23°C during all tests. All the specimens were heated for 2 minutes from the back side, and the black plate was used to protect the camera. The OPTRIS PI connect software was employed to capture the IR images during the cooling process.

Results and discussions

Physical properties analysis

The total thicknesses, total weight, fiber weight fraction, and metal volume fraction (MVF) of three hybrid laminates are displayed in Table 1. The weight of the aluminum sheet in ACPCA and CAPAC is 195 g and 196 g, respectively. Moreover, the carbon fiber mass in CPC, ACPCA, and CAPAC is 39.21 g, 40 g, and 38.21 g, respectively. The P mass in CPC, ACPCA, and CAPAC is 24.5 g, 24.8 g, and 24.45 g, respectively. The total fiber weight fraction of hybrid FRP composite is 38%, while the hybrid FMLs is approximately

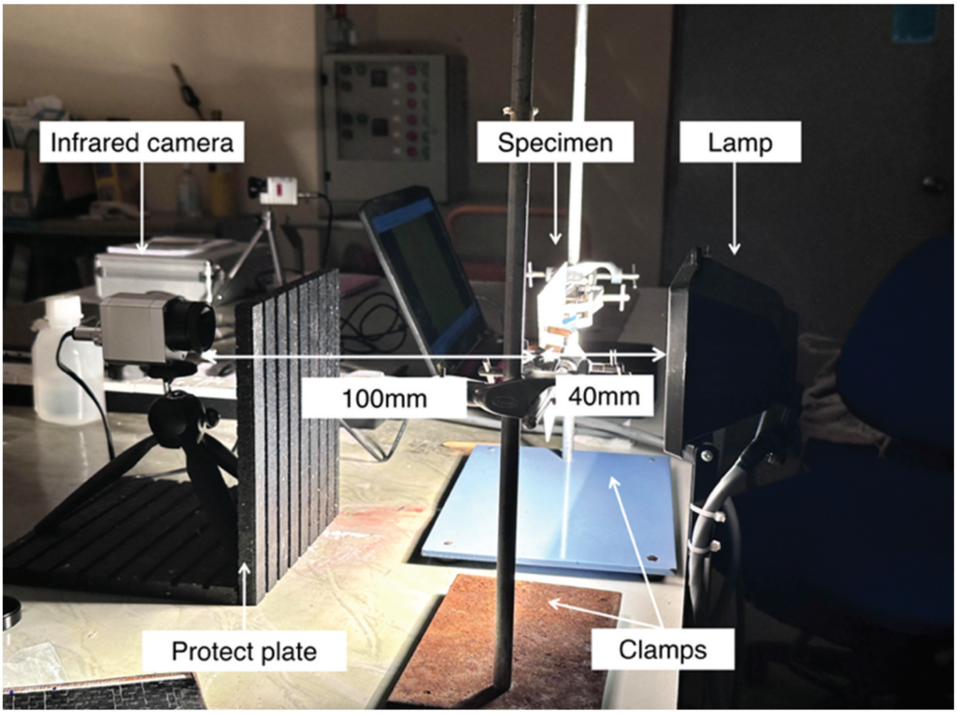

Figure 5. The setup of the infrared thermography test of hybrid composites.

Table 1. Physical properties of three hybrid laminates.

Sample	Total thickness (mm)	Total weight (g)	Fiber weight fraction (%) C	P	Total	Metal volume fraction (%)
ACPCA	2.12	349.98	11.43	37.74	18.52	37.74
CAPAC	2.23	359.62	10.63	35.87	17.43	35.87
CPC	1.31	168.34	23.29	14.55	37.84	0

18%. The fiber weight fraction of the CPC composites is higher than that of the hybrid FMLs since CPC lacks the A sheet that promotes the fiber's absorption of the resin during the VARTM process.

Flexural test analysis

The material will undergo bending stress as a result of an impact. Therefore, bending characteristics can indicate a composite's potential impact strength characteristics (Najeeb et al. 2021). However, little research has been done on the relationship between flexural and impact strengths of the hybrid composites, and how FMLs and FRP composites behave differently. This research determined the bending properties of hybrid composites through flexural tests. The flexural stress–strain curves of three hybrid composites are displayed in Figure 6. The average flexural strength and flexural modulus are shown in Figure 7. The results indicate that the FRP composite CPC exhibits significantly higher flexural properties than the two hybrid FMLs, ACPCA and CAPAC. CPC's average flexural strength and strain is 545.07 MPa and 63.26 GPa, respectively, indicate its high flexural properties. After reaching peak flexural stress, CPC experiences a dramatic stress reduction, indicating cracking due to its brittleness. The CPC's strength is derived from its fiber-reinforced structure, providing a high strength-to-weight ratio, though it exhibits brittleness, as evidenced by a dramatic stress reduction

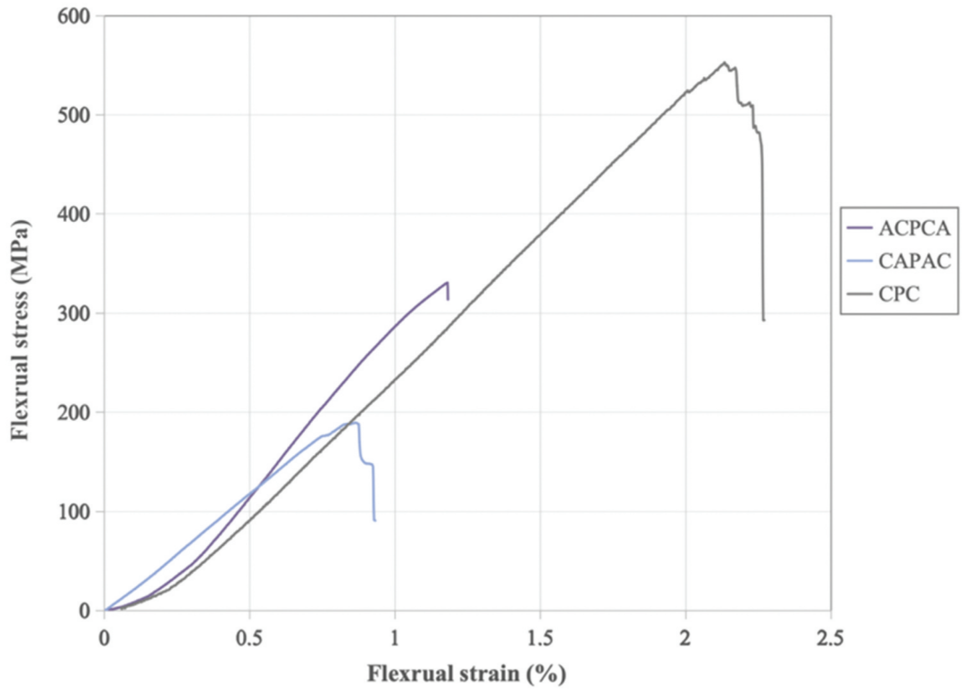

Figure 6. Flexural stress–strain curves of hybrid laminates CPC, ACPCA, CAPAC.

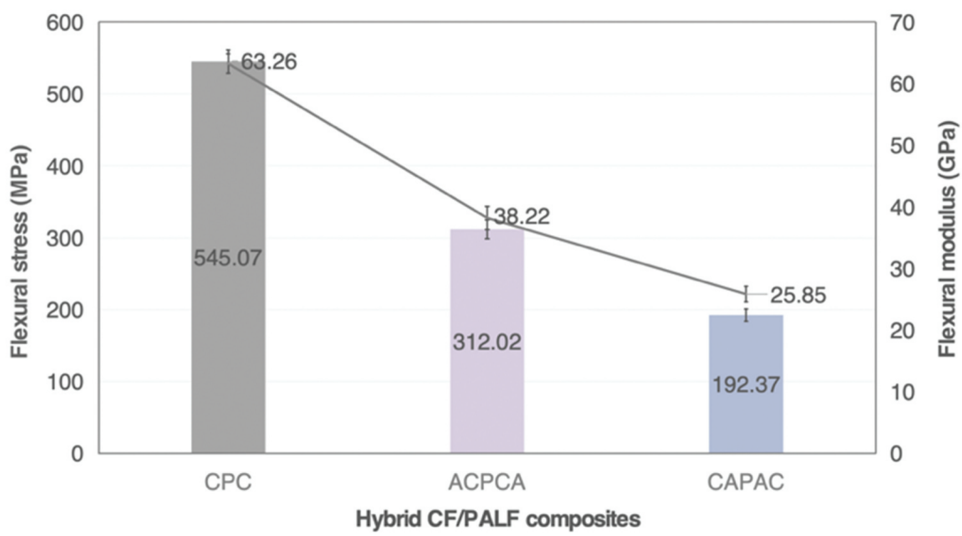

Figure 7. Flexural stress and modulus results of hybrid laminates CPC, ACPCA, CAPAC.

upon cracking. In contrast, hybrid FMLs like ACPCA and CAPAC incorporate aluminum layers, leading to early delamination under flexural loads. This delamination is caused by stress concentrations from the differing material properties between aluminum and FRP layers, resulting in separation and reduced deformation capacity under flexural loads. The poor bonding between aluminum and FRP further exacerbates this issue, leading to earlier failure and reduced capacity to endure deformation. These findings highlight that delamination between metal and FRP layers is a critical failure mode in FMLs (Wu et al. 2020; Yanyan et al. 2020), making them more rigid and less flexible than pure FRP composites. Factors like aluminum surface treatments and resin compatibility further influence the initiation and propagation of delamination, which should be addressed in future work.

When comparing the two hybrid FMLs, the FMLs ACPCA placing aluminum as the outer layer demonstrates better flexural performance than CAPAC. As illustrated in Figure 6, the flexural strength of ACPCA is 312.02 MPa, which is a 62.2% improvement compared to CAPAC, which is 192.37 MPa only. This enhancement occurs primarily because placing ductile aluminum on the outside helps distribute stress more uniformly, absorbing energy and expanding the deformation zone, which enables ACPCA to withstand higher flexural loads. The configuration ACPCA also minimizes the direct exposure of brittle carbon fiber layers to stress, enhancing the overall structural integrity of the laminate. Moreover, the outside aluminum layer in ACPCA mitigates delamination between layers, a critical failure mode in FMLs, whereas CAPAC, with internal aluminum, may experience more severe delamination due to weak bonding with adjacent composite layers under flexural stress. These findings are consistent with research from Hynes et al. (2022), which demonstrated that ACACA specimens that placing AA6061 plates at the outer end have a higher ultimate breaking load of approximately 155 N compared to 120 N for CACAC during flexural testing, and a maximum displacement of 11.10 mm compared to approximately 8 mm for CACAC.

LVI test analysis

The LVI testing aims to assess the impact damage behavior before total perforation for each hybrid laminate. The impact energies were determined based on previous research for FRP composites with three layers. Following Imran et al.'s study (Najeeb et al. 2021), which explored impact energies from 2 J to 9 J for hybrid GPG composites, our experimental approach initially set at 5 J impact energy. At this energy level, the CPC composite already displayed noticeable cracking, and by 10 J, it had completely failed. This indicated that further analyze at 10 J was redundant as the sample was already fully compromised. In order to better understand early damage in CPC, we reduced the impact energies to 2 J and 1 J. Consequently, the CPC composites were subjected to impact drop height at 20 mm, 40 mm, 100 mm, and 200 mm, corresponding to 1.0 J, 2.0 J, 5.0 J, and 10.0 J of energy, respectively. For FMLs, both FMLs did not show significant delamination or damage at 5 J, leading us to increase the impact energy to 10 J and eventually to 15 J, where clear material failure was observed. The tests were carried out at 100 mm, 200 mm, and 300 mm drop heights for FMLs ACPCA and CAPAC, corresponding to 5.0 J, 10.0 J, and 15.0 J of energy, respectively. This stepwise approach allowed for a detailed assessment of impact responses and failure modes for both FMLs and CPC across various energy levels, ensuring a comprehensive evaluation of their performance.

Comparison of peak force

The peak force (F_{peak}) in the force–displacement curve of a tested material is a crucial parameter, representing the highest loading the materials can bear before failing during impact. The F_{peak} of three hybrid composites is displayed in Figure 8. The highest peak force values of ACPCA and CAPAC were recorded at 2.71 kN and 2.29 kN, respectively, compared to CPC of 0.74 kN, showcasing a 266.22% and 209.50% improvement in impact resistance, respectively. This is because the aluminum sheets aid in improving impact damage resistance by metal ductile deformation and lowering local damage from the point of impact. This finding aligns with other studies that stated the enhanced impact characteristics of FMLs compared to pure FRP composites (Koh-Dzul et al. 2023; Xiao, Sultan, Shahar, Gaff, et al. 2023; Zhang et al. 2023). In addition, the maximum peak force of the ACPCA of 2.71 kN was 18.34% greater than the CAPAC of 2.29 kN. As illustrated in Figure 8, the peak force value of ACPCA continues to rise with an increase in impact energy at 5–15 J. In contrast, the peak force value of CAPAC appears at 10 J impact energy

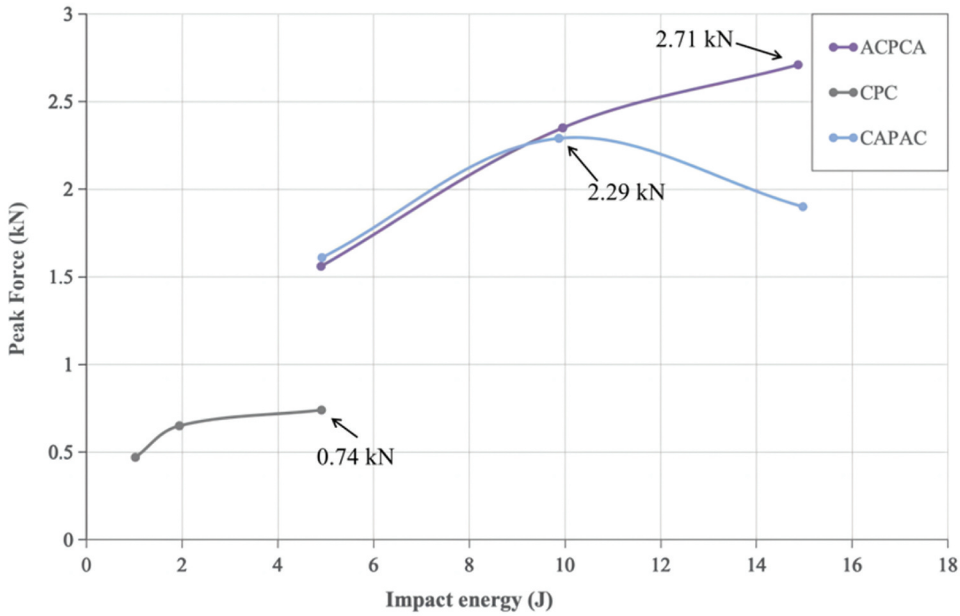

Figure 8. Peak force of hybrid composites.

and decreases at 15J impact energy. This means the hybrid FMLs placing A as outer layer withstand much higher impact energy than FMLs insert the A inside the composites because the plastic deformation of the aluminum sheet served as the primary energy dissipation factor. Zhang et al. (2022) also noted a similar case, and they pointed out that plastic deformation of the aluminum layers was the primary mechanism for energy dissipation of hybrid A/C laminates. Placing A layers on the outer surface enhanced the absorption of impact energy and mitigated the fracture behavior of the component layers.

Comparison of force–displacement curve

Figure 9 compares force–displacement curves of the highest impact energy before perforation. The LVI testing showed that the composite CPC can only withstand a maximum impact force of 5 J while it is totally broken under 10 J of impact force. Meanwhile, ACPCA and CAPAC have an impact resistance of up to 15 J before perforation, indicating they can withstand LVI at least 200% higher than composite CPC. F_{peak} is associated with the highest resistance point during impact in force–displacement curves. As shown in Figure 9, the F_{peak} of ACPCA is higher than CAPAC and much higher than CPC. In addition, the slope in the crack initiation zone of the graph represented the stiffness property of the materials. From the comparison curve, the CPC has a significantly lower stiffness property than the other two FMLs. This suggests that the CPC is the most brittle of the FMLs composites due to the absence of metal layers. The open loop CPC graph supported this conclusion, while the two other variations had rebound behavior. The open loop curve of the metal-free composite CPC during LVI testing indicates that FMLs have better elasticity qualities than the composite CPC. In addition, the partial rebound behavior of FMLs CAPAC means that a part of the impact force is used for deformation in the perforation, and a portion is used for cracking and distortion in the rebound. However, at the same impact energy of 15 J, the FMLs ACPCA still displayed fully rebound behavior. The comparison results highlights that the FMLs incorporated with A layers have much better impact resistance than CPC composites without A layers, and placing A as outer layers further improves impact resistance. Xiao et al. (2024) demonstrated that the hybrid FMLs ACPCA significantly

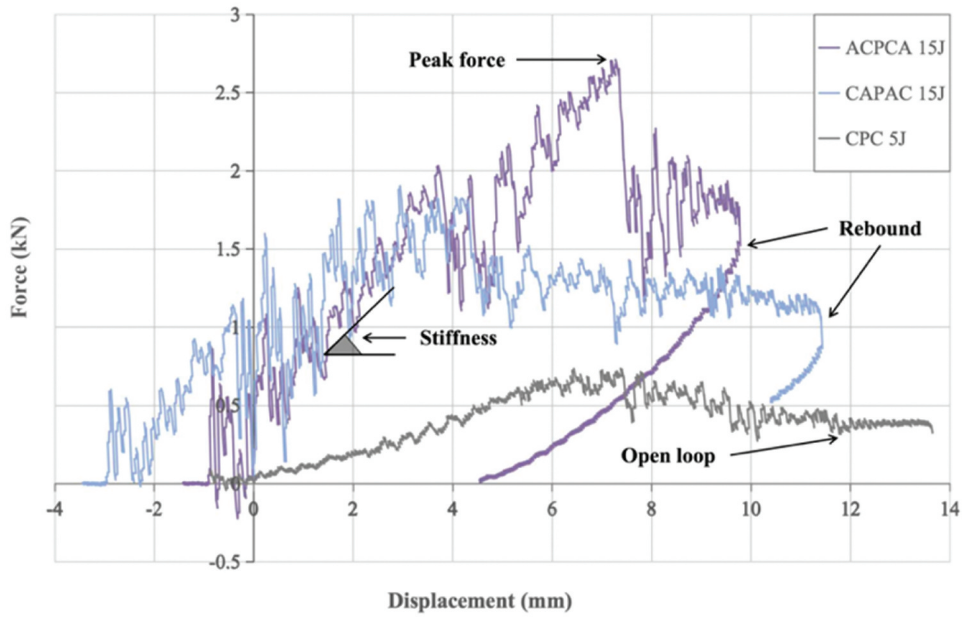

Figure 9. Force–displacement curves of maximum impact energy prior to composites perforation.

outperformed CPAPC, achieving 83.51% higher ILSS and 75.34% greater Izod impact strength. This research reinforces that positioning A as the outer layer in FMLs enhances impact resistance of FMLs.

Force–displacement curve of CPC. Figures 10–12 show three variations of the LVI force–displacement curve at different energy levels. As shown in Figure 10, CPC shows the rebound behavior at very low energy 1 J and 2 J, where the applied force of CPC increased correspondingly with the

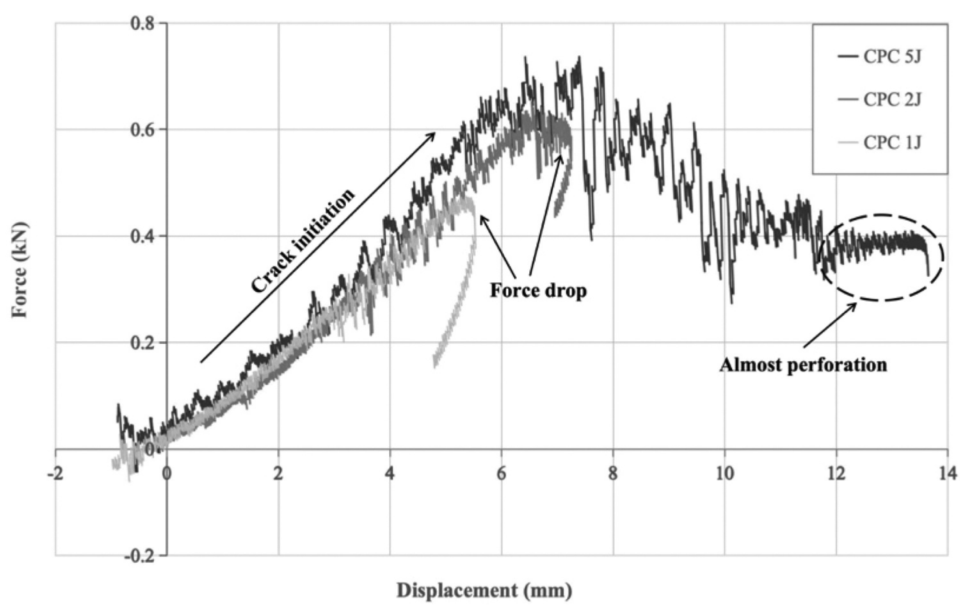

Figure 10. Force–displacement curves of different impact energy on CPC (without Al).

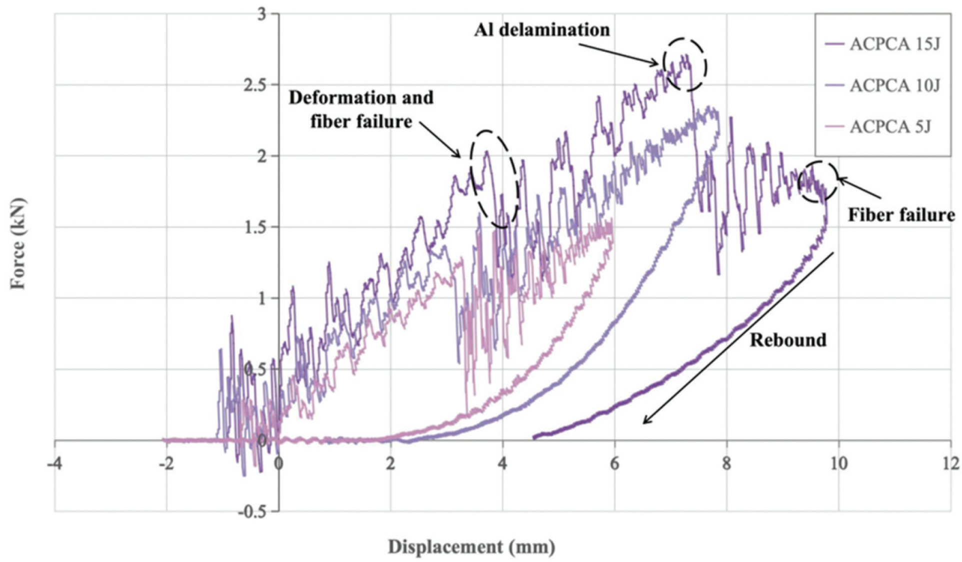

Figure 11. Force–displacement curves of impact energy before ACPCA perforation.

displacement till it reached a F_{peak} and had a sudden force drop. The proportional increment characteristic is due to the vibrating movement between the specimen and the impactor. The sudden force drop is due to the high strength of the C hybrid with P. Even if the FRP composite is brittle, it can still withstand low-impact energy. However, the force–displacement curve of the CPC composite changed to a fully open loop because the low stiffness, and the composites almost perforated at an impact energy of 5 J. A similar force–displacement curve pattern with P hybrid G composites (GPG) was reported by Imran et al. (Najeeb et al. 2021). At lower impact energies, the GPG curve displays a sharp decline in impact force after reaching its peak. At higher impact energies, the curve also

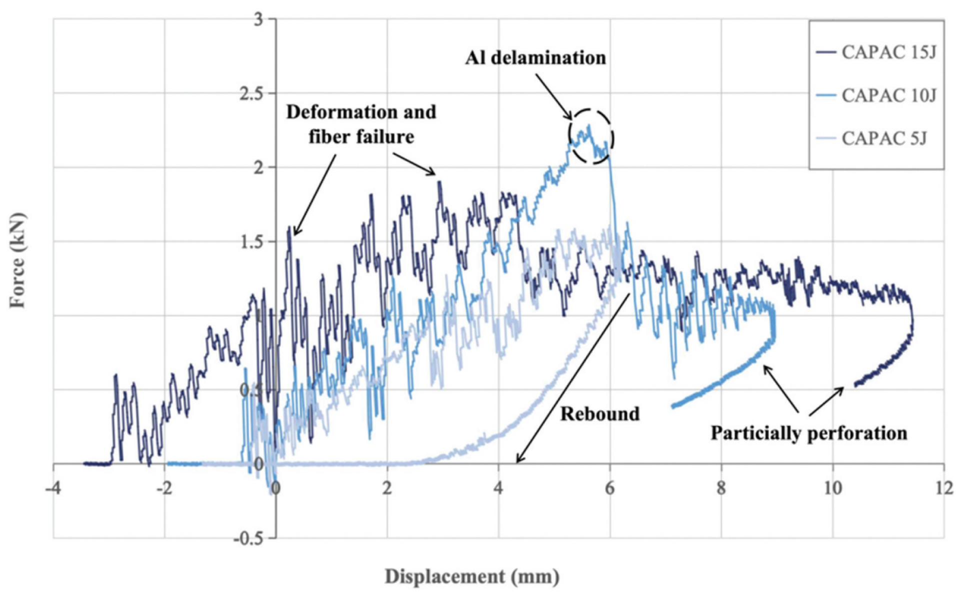

Figure 12. Force–displacement curves of impact energy before CAPAC perforation.

exhibits an open-loop pattern: it first drops after reaching the initial peak force and then gradually elongated as the composite resists further penetration by the striker.

Force–displacement curve of ACPCA. For hybrid FMLs ACPCA, the force–displacement curve (Figure 11) shows that all the composites took the rebound upon impact energy with 5–15 J, and a greater area is covered beneath the curve as the impact energy increases. According to Imran et al. (Najeeb et al. 2021), the area under the curve represents the deformation energy throughout the energy recovery process. When an impactor strikes a material, energy transfers from the impactor to the specimen, causing deformation. This deformation energy, shown by the area under the curve, is used to overcome the material's resistance, resulting in changes such as bending, stretching, or cracking. Consequently, as the impact energy increases, the area under the curve also increases. From the graph, all the samples show a linear force increment at the initial stage, then drop around 3 mm-4 mm displacement before reaching the peak force. Matrix cracking, metal deformation, and fiber failure usually happen in this period. This behavior mirrors the findings of Hussain et al. (2022), who reported similar force–displacement curve patterns for their hybrid A/C/jute fiber/epoxy (ACJCA) composites, where matrix cracking, metal deformation, and fiber failure may occurred before reaching the peak force during LVI testing. After reaching the peak force F_{peak}, the specimen ACPCA under 5 J and 10 J shows a sharp impact force drop and then returns to the initial point. This means the composites were fully rebound after impact without future failure. However, the specimen under 15 J impact energy has the second sharp force drop after reaching the Fpeak and then decreases somewhat gradually with increasing displacement. These results show that 15 J is high enough to trigger more fiber failure and delamination for ACPCA.

Force–displacement curve of CAPAC. Compared with the hybrid FMLs ACPCA, CAPAC shows lower impact resistance. At a lower impact energy of 5 J, the same graph trend as ACPCA was observed in CAPAC as rebound behavior. There is a linear force increment until the sharp impact force decreases and returns to the initial point. However, the curve of CAPAC at 10 J impact energy has a similar trend with the ACPCA at 15 J impact energy, which means the CAPAC can stand lower impact energy than ACPCA. The reason may be because the outer layer is the leading loading of the impact force. Placing brittle C as an outer layer lowers the stiffness of the whole composites, thus leading to lower impact resistance. In addition, the F_{peak} of CAPAC at a high-impact energy of 15 J is lower than the F_{peak} of CAPAC at energy of 10 J. As Figure 12 illustrates, a big saw was observed in the CAPAC curve before F_{peak} at a high impact energy of 15 J. It can be inferred that under the high impact energy, the outer C layers of CAPAC partially fails before F_{peak}, thus reducing the value of F_{peak}. In addition, after the F_{peak} was reached, the curve kept getting longer. It showed a gradual increase in impact force after an apparent decline due to the resistance of the inner A layers, which keeps the striker from perforating the composites. The curve still shows rebound behavior because the inner Al effectively stops the striker impact. These results were also supported in A/G laminates researched by Zhang et al. (2023), where the plastic and elastic energy account for roughly 70% of the total energy dissipation at the beginning of LVI. In contrast, the unrecovered elastic strain energy for GF reinforced composites only accounts for around 20% of the final stored energy. These results proved that aluminum layers play a more significant role than FRP in FMLs, influencing the damage evolution and rebounding processes.

Comparison of energy-time

The typical energy-time of the impact event is shown in Figure 13a. The difference between the impact and absorbed energies subsequently determines the rebound energy in terms of rebound behavior. Thus, there are two sections to the energy–time curve: (1) upwards to impact energy and (2) downward to absorbed energy. While the remaining energy is retained as elastic energy, resulting in a rebound, and is returned to the impactor, the absorbed energy is used for deformation. The more absorbed energy, the more deformation happens inside the materials. If the sample were perforated or

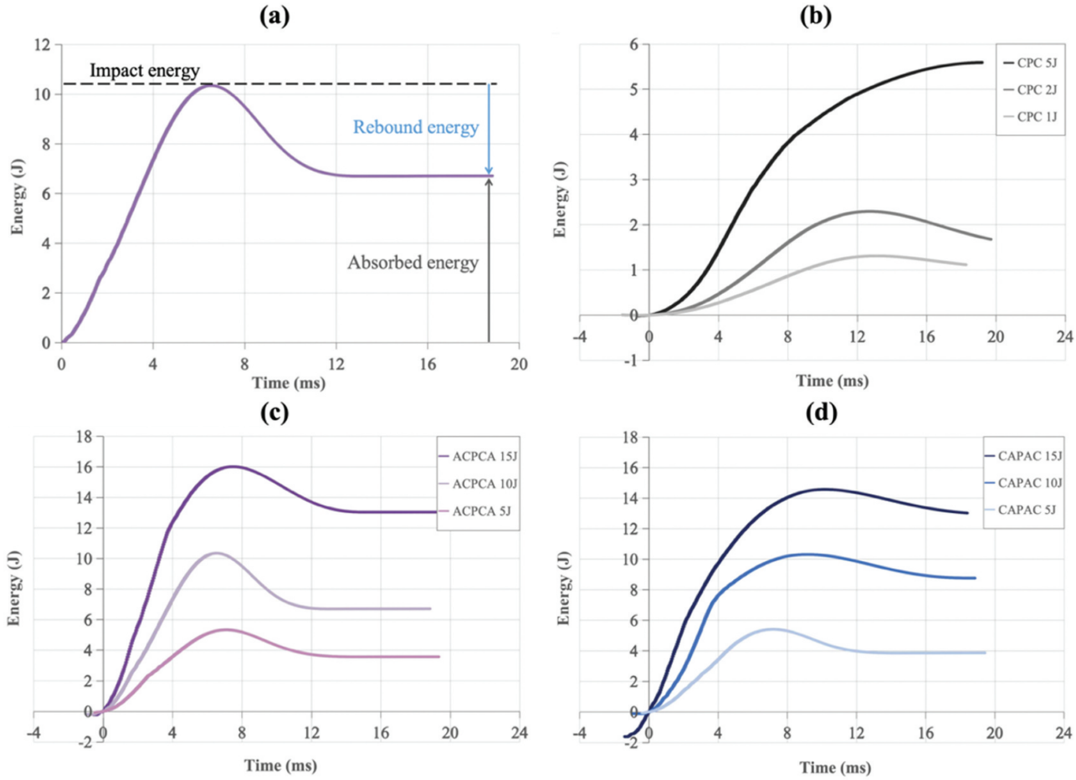

Figure 13. The energy–time curves of composites (a) the typical energy-time of the impact event (b) CPC composites (c) hybrid FMLs ACPCA (d) hybrid FMLs CAPAC.

near failure, the sample would absorb all the impact energy. The energy–time curves for all three hybrid laminates at different impact energies are shown in Figures 13b–d. The energy–time curves of the CPC composite at 5 J (Figure 13b) demonstrate that for the near perforation, almost all the impact energy is utilized for specimen deformation. This is consistent with the open loop curve results of the CPC composite at 5 J impact energy in the force-displacement curve (Figure 10), which demonstrated that the CPC composite did not undergo rebound behavior at 5 J impact energy, that is why the impact energy and absorbed energy are equivalent.

Compared with the composites CPC, the FMLs ACPCA and CAPAC displayed the maximum energy before decreasing to a constant energy under all the impact energy 5 J, 10 J, and 15 J in both Figure 13c,d. The constant energy indicates the energy the specimens have dissipated, and the highest peak represents the impact energy (Najeeb et al. 2021). It should be noted that at 5 J, the ACPCA and CAPAC displayed similar energy–time curves, which had fully rebounded. Whereas the CAPAC absorbed more energy than ACPCA at a higher impact energy of 10 J and 15 J, there is more inner deformation, fiber failure, delamination, or other failure mechanism in CAPAC at high energy. In addition, under a higher impact energy of 15 J, the CAPAC had a more prolonged time to reach the peak energy than the ACPCA, averaging 10.17 ms versus 7.48 ms respectively. This displays that the CAPAC layering sequence reduced the time needed for damage to start and spread throughout the specimen because the brittle carbon fiber got exposed and dissipated the energy by FRP failure. These results align with the research on C/A laminates from Zhang et al. (2022). They discovered that the energy dissipation of FMLs with carbon fiber layers as skin sheets was mainly triggered by FRP cracking and delamination, which showed more extensive delamination regions and more intense breakage behavior than FMLs with A layers as skin sheets.

Correlation between flexural and impact performance

The bending and impact performance of the three samples demonstrate a strong correlation between their structural integrity under bending loads and their response to impact energies. Samples that withstand bending loads well tend to show better resistance to low-energy impacts. However, as the impact energy increases, the extent of damage under bending loads becomes more pronounced, indicating a direct relationship between bending-induced damage mechanisms and impact resistance. Figure 7 shows that CPC, with a flexural strength of 545.07 MPa and a flexural modulus of 63.26 GPa, demonstrates superior bending performance. However, despite its high bending strength, CPC exhibits a lower perforation energy of 5 J and a peak force of 0.74 kN, indicating that it is less capable of withstanding high-impact energies. This suggests that while CPC performs well under bending loads, it is prone to early damage under impact. This aligns with the observation that CPC composites start to show damage at 5 J impact energy, with crack propagation occurring at higher energies.

ACPAC samples show moderate bending strength of 312.02 MPa and stiffness of 38.22 GPa. However, when evaluating its impact performance, ACPAC shows a better capacity to absorb impact energy before perforation occurs, with a perforation energy of 15 J and a peak force of 2.71 kN. This indicates that ACPAC maintains a balance between bending strength and impact resistance, allowing it to withstand higher impact energies compared to CPC. In addition, when comparing the two hybrid FMLs, the FMLs ACPCA placing aluminum as the outer layer showed better flexural performance and LVI behavior than CAPAC. CAPAC has a lower flexural stress of 192.37 MPa and a flexural modulus of 25.85 GPa, while the flexural strength of ACPCA is a 62.2% improvement compared to CAPAC. In terms of impact performance, CAPAC has a perforation energy of 10 J and a peak force of 2.29 kN. CAPAC shows significant damage at 10 J and 15 J impact energies, including more pronounced inner deformation and delamination. This aligns with its lower bending performance, placing A as the outer layer widened the plastic zone of the FMLs, indicating that CAPAC struggles to withstand both bending and impact loads.

In summary, the correlation between bending and impact performance suggests that samples with higher bending strength and stiffness (CPC) tend to show better resistance to bending loads but may not necessarily perform well under high-impact energies. Conversely, hybrid FMLs ACPAC, with moderate bending performance, can absorb higher impact energies before significant damage occurs, suggesting a balance between bending and impact resistance. This correlation underscores the importance of considering both bending and impact performance in evaluating the overall durability and suitability of composite materials.

Visual inspection

The visual inspection of hybrid composites under different impact energy is shown in Figures 14–16. From the visual inspection, obvious cracks and delamination appeared in CPC with 5 J, ACPCA with 15 J, and CAPAC with 15 J, respectively. Thus, the maximum impact energy before perforation for CPC, ACPCA, and CAPAC were limited to 5 J, 15 J, and 15 J, respectively.

In Figure 14, the hybrid composite CPC had no apparent visual damage under impact energy of 1 J and 2 J because the hybrid fibers can withstand some extent of impact force. However, cracks appeared in CPC composites along the center line (C direction) at 5 J of impact energy, and the specimen was totally broken under 10 J impact energy. The damage feature indicated that the CPC composites exhibited brittle fracture performance without ductile A layers. Moreover, fiber orientation significantly affects the strength and stiffness of the laminates, which can in turn influence its impact performance. The unidirectional CF causes the resin-poor area of CPC composites, which is why the straight vertical damaged line formed after the LVI test. Lee et al. (2018) also emphasized layering architecture's crucial role in determining the composite laminates' low-velocity impact behavior. They highlight the effect of fiber orientation in determining the direction of crack

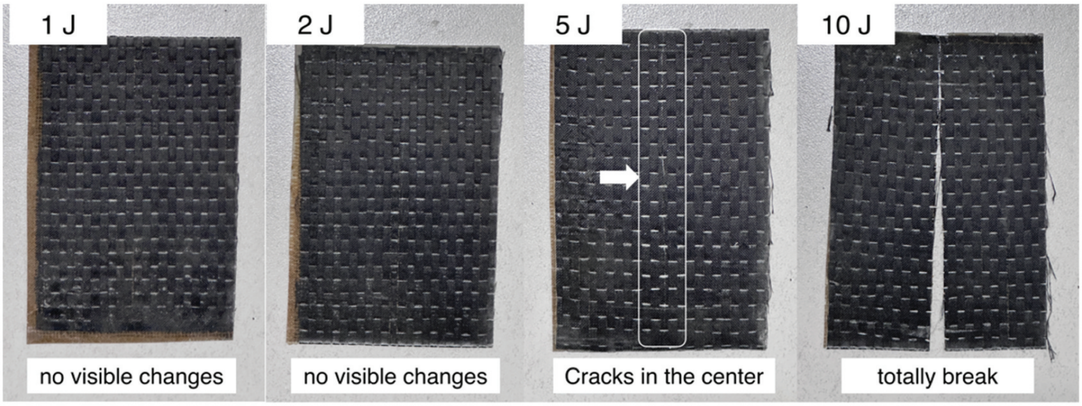

Figure 14. Visual inspection of impacted CPC at various impact energies.

propagation during LVI testing. These findings align with the LVI test results. The CPC composites display an open loop in the force-displacement curve at 5 J, and almost all the impact energy is absorbed in the energy–time curve, suggesting that the material rapidly reaches its failure point without significant plastic deformation.

The failure evolution of hybrid FMLs ACPCA and CAPAC have different failure changes than FRP composite CPC. For specimen ACPCA, the cracking is not observed in the impact face (top face) or bottom face under 5 J and 10 J, but the crack appears in the bottom A layer with 15 J impact energy. In addition, these results align with the force–displacement curve in Figure 11. The specimen fully rebounds after impact without future failure under 5 J and 10 J. At the same time, there is the second sharp force drop after F_{peak}, which decreases somewhat gradually with increasing displacement under 15 J impact energy because more fiber failure and delamination happen. The visual damage evolution performance of the impacted CAPAC specimens also corresponds with the LVI test results. Under 5 J impact energy, CAPAC has no visible cracks and delamination. Thus, the force–displacement curve in Figure 13 exhibited a closed loop, representing rebound behavior. When the impact energy increased to 10 J, visible delamination could be seen, but no crack appeared either in the impact or bottom face. Thus, the force-displacement curve had a similar trend to the ACPCA curve under 15 J. Until the impact energy of 15 J, the crack appeared in the center of the impact face, and significant delamination can be seen. These results again aligned with the force–displacement curve in Figure 13, where the curve shows rebound behavior because the inner Al effectively stops the striker from perforating the composites. However, for CAPAC, the high impact energy result in outer C layers crack and significant delamination, and that is why the big saw can be seen before the F_{peak}. From these results, the visual inspection results align with the previous research (Sharma et al. 2018), the damage and delamination became more severe with the increase in energy impact. In addition, the different damage evolution of hybrid FMLs ACPCA and CAPAC mainly due to the layering sequence. The specific arrangement of these layers can significantly influence the material's response to impact forces because of the different mechanical properties of the metal and FRP layers, where metals typically provide strength and toughness, while composites offer high stiffness and lower density.

Infrared thermography test

The visual inspections are still limited in the extent to which the actual extent of the damage can be measured. In order to obtain more accurate and reliable results to evaluate the damage mechanism during the LVI test, it is usually necessary to combine other detection methods. In this study, infrared thermography (IR), a representative nondestructive detection method, was used to observe the

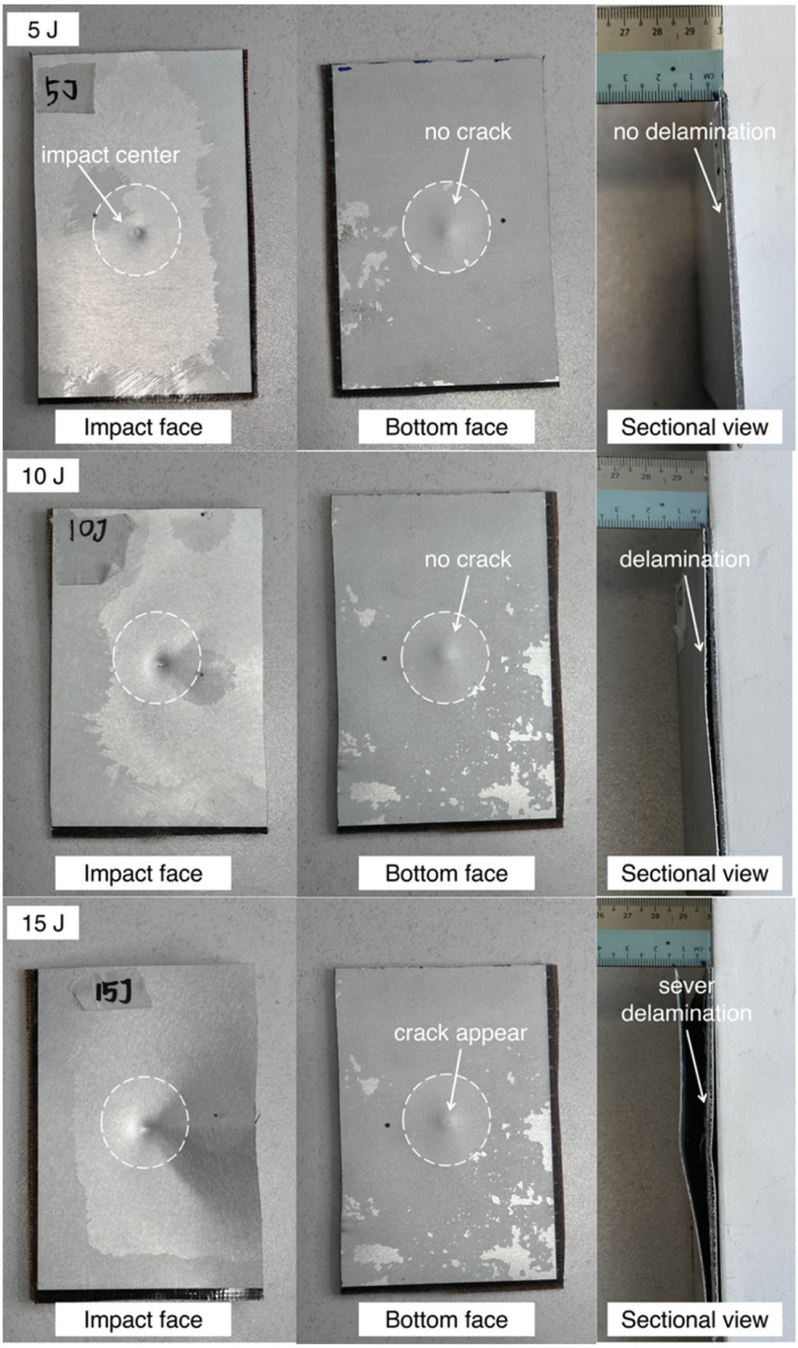

Figure 15. Visual inspection of impacted ACPCA at various impact energy.

damaged area of three composite materials under the LVI. The images obtained from the IR test are shown in Figure 17.

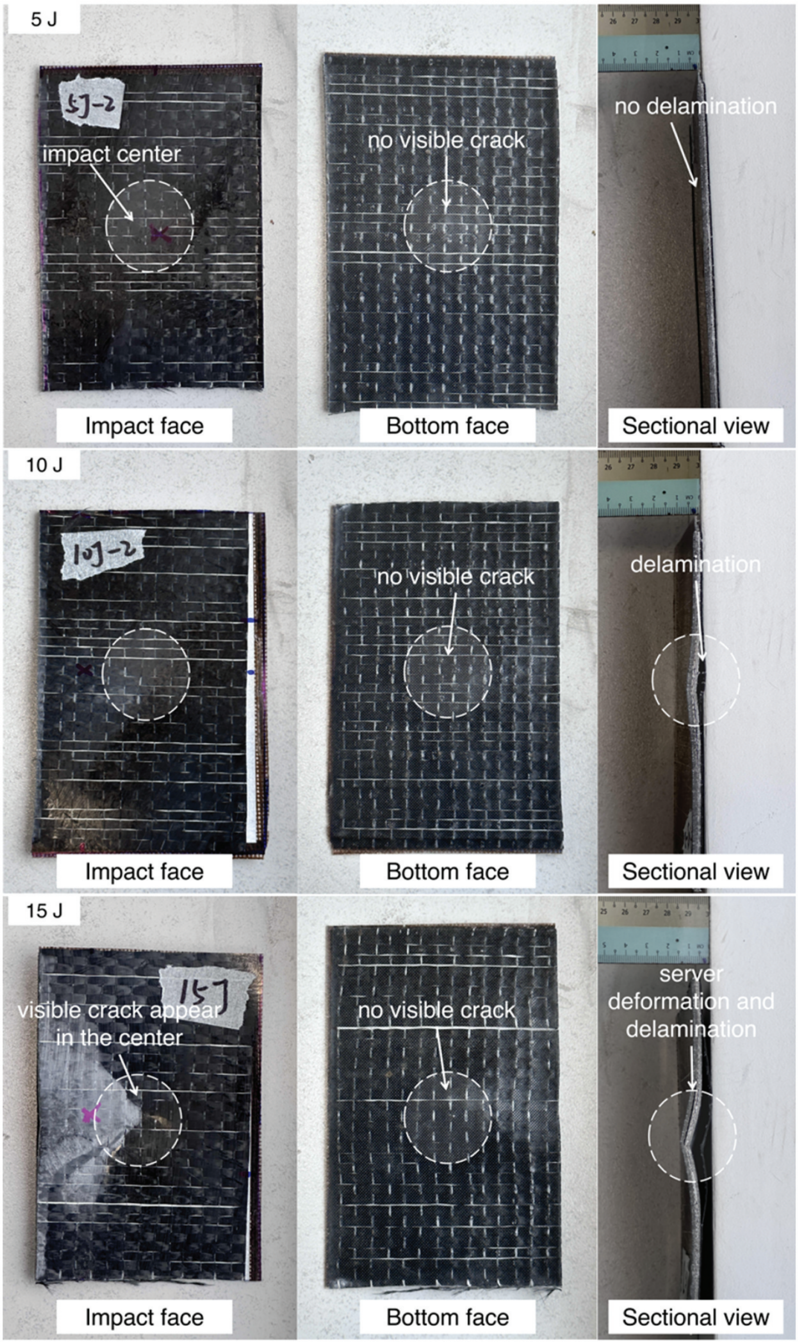

Figure 16. Visual inspection of impacted CAPAC at various impact energy.

IR results of CPC

As illustrated in Figure 17a, no damage was captured in CPC composites subjected to 1 J and 2 J due to the limitation of the equipment. This phenomenon indicated that the hybrid C/P composites can absorb the impact force at lower impact energy ranges. Thus, the damage of CPC composites cannot be captured at 1 J and 2 J in IR images. The IR results correspond with the visual inspection, as shown

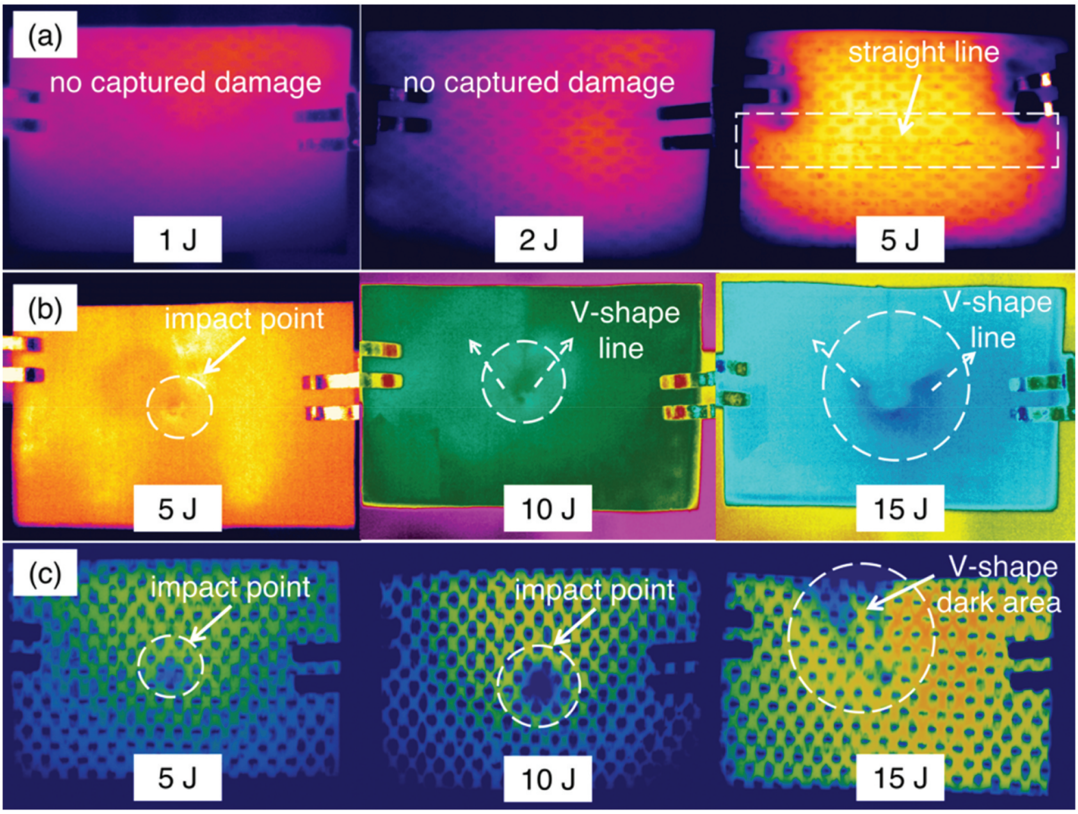

Figure 17. IR results of hybrid composites after low-velocity impact. (a) hybrid FRP CPC (b) hybrid FMLs ACPCA (c) hybrid FMLs CAPAC.

in Figure 14. However, a horizontal straight line was observed when the CPC composites were subjected to 5J impact energy. The infrared image reveals that the crack is situated near the impact center on the specimen, extending along the unidirectional C direction within the composite. This observation again aligns with the visual findings depicted in Figure 14. The longitudinal cracks witnessed in CF-reinforced epoxy also propagated along the C direction, as previously reported by Ma, Y. et al. (2021).

IR results of ACPCA

Figure 17b shows the damage area revolution of ACPCA under different impact energy. At 5 J impact energy, there is apparent circular local damage at the center of the specimen, which was formed during the LVI process. In the vicinity of the impact point, other than the bright area caused by the reflection of the aluminum alloy, no other noticeable damage features were found. When ACPAC is exposed to 10 J impact energy, the infrared image enlarges the circular dark area at the central point, signifying an increased scope of local damage in that region. The IR image exhibits a significant contrast component owing to the specimen's varying degrees of matrix cracking, fiber breakage, delamination and deformation due to the dissipation of energy as heat, which differ in the defect area. Figure 17b also shows three darker lines extending from the circular damage point to the sample boundary, which are evident. This dark triangular area results from the noticeable deformation and delamination of the composites under LVI. Furthermore, a larger circular area and a broader triangular region of the sample can be seen when ACPCA is subjected to 15 J impact energy, indicating a continued increase in internal damage, deformation, and delamination. The IR results correspond with the force–displacement curves in Figures 11 and 12, where the severe delamination and deformation represented by a large, abrupt drop in force, indicating a significant loss of structural integrity.

IR results of CAPAC

The damage revolution in the hybrid FMLs CAPAC exhibits a similar trend to the ACPCA. As shown in Figure 17c, more significant damage is induced in CAPAC by higher impact energies. These findings also align with the visual observations in Figure 16. When exposed to an impact energy of 5 J, it experienced concentrated damage at the center, similar to ACPCA. The IR test shows no significant delamination and deformation, and the results are the same as the visual inspection of Figure 16. When the specimen was exposed to an impact energy of 10 J, the area of damage increased. It should be noted that the CAPAC did not display the V-shape era under 10 J impact energy. The difference is that CAPAC utilized C as outer layers while ACPCA utilized A as outer layers. When the high stiffness carbon fiber is the outer layer of CAPAC, the outer FRP may break first and present as a barrier from further composite deformation. As a result, the IR image of CAPAC under 10 J is not as significant as the ACPAC image under 10 J. When subjected to 15 J impact energy, a clear view of delamination and deformation can be seen (V-shape dark aera). These results align with the energy–time curve in Figure 13, where the CAPAC absorbed more energy than ACPAC at a higher impact energy.

Conclusions

In this study, we investigated the flexural and LVI behavior of three hybrid laminates (CPC, ACPAC, CAPAC) composed of C/P reinforced epoxy. According to the reported variations in the flexural and LVI characteristics, the hybrid FMLs demonstrated increased rigidity and superior impact resistance compared to the FRP composite (CPC), and the hybrid FMLs ACPCA is more resistant to impacts than CAPAC. The addition of an aluminum layer and its sequence in the laminate significantly influenced the impact properties and flexural characteristics. In particular, the flexural tests reveal that the hybrid fiber-reinforced polymer (FRP) composite CPC demonstrates superior flexural properties than other FMLs, with an average flexural strength of 545.07 MPa and a strain of 63.26%. In comparison, the hybrid FMLs ACPCA exhibit intermediate flexural strength (312.02 MPa) among the three laminates, showing a 62.2% improvement over the FMLs CAPAC (192.37 MPa). From LVI test results, adding A layer as skin sheets of the composite (ACPCA) demonstrates a 266.22% higher F_{peak} (2.71 kN) value than CPC (0.74 kN). At a high impact energy of 15 J, the outer CF layers failed prior to the F_{peak}, which means the CAPAC absorbed more energy than the ACPCA and produced a partial rebound in the force–displacement curve for the CAPAC, while a full rebound curve for the ACPCA. The LVI test results are almost aligned with the visual inspection and the IR technique. It was shown that CPC cannot capture apparent damage with the naked eye and IR technology at low energy impact, while at high energy 5 J, penetrating cracks along the fiber direction are directly observed. The damage range of FMLs grows with the increase of impact energy and shows V-type damage at higher energy levels, indicating that more severe delamination occurs there.

In conclusion, from a cost-effectiveness perspective, the P used in this research, sourced from agricultural waste, offers a more economical and environmentally friendly alternative to fully synthetic fiber-reinforced laminates. Additionally, low density of P results in lower energy consumption and further cost savings. This research highlights the importance of considering both bending and impact performance when evaluating the structural integrity and durability of composite materials. The results of this study suggest that the hybrid FMLs ACPAC, which balance bending and impact resistance, could be beneficially utilized in automotive applications requiring high rigidity and impact resistance, such as car bumpers and door panels. However, a significant limitation of the study is the issue of delamination in hybrid FMLs, which can impair their flexibility and impact properties, reducing practical effectiveness. Future research should focus on preventing delamination to improve the performance and economic viability of these laminates.

Acknowledgments

The authors would like to thank the Department of Aerospace Engineering, Faculty of Engineering, Universiti Putra Malaysia, and Laboratory of Biocomposite Technology, Institute of Tropical Forestry and Forest Product (INTROP), Universiti Putra Malaysia, for the close collaboration in this research.

Disclosure statement

No potential conflict of interest was reported by the authors.

Funding

The authors would like to thank Universiti Putra Malaysia for the financial support through Geran Inisiatif Putra Siswazah (GP-IPS) with grant number 9739200.

ORCID

Mohamed Thariq Hameed Sultan http://orcid.org/0000-0002-5110-0242

Author contributions

Conceptualization, HX; methodology, HX; formal analysis, HX; investigation, HX; resources, MTHS; data curation, HX; writing – original draft preparation, HX; writing – review and editing, MTHS, FSS, and SYN; Visualization, HX; supervision, MTHS and SYN; project administration, FSS, and SYN; funding acquisition, MTHS, and SYN. All authors have read and agreed to the published version of the manuscript.

Data availability statement

The authors confirm that the data supporting the findings of this study are available within the article.

Highlights

(1) The impact failure behaviors of three hybrid laminates based on carbon fiber (C)/pineapple leaf fiber (P) were researched through a low-velocity impact (LVI) test.
(2) The effect of the addition of aluminum (A) and A layer position in all hybrid laminates were investigated by flexural test, peak force, force–displacement curves, energy–time curves, visual inspection, and infrared thermography (IR) tests.
(3) The results highlight that the hybrid FMLs ACPCA can be used in automotive applications where impact resistance is critical, such as the car bumper and door panels.

References

Abd El-Baky, M. A., A. E. Alshorbagy, A. M. Alsaeedy, and M. Megahed. 2022. “Fabrication of Cost Effective Fiber Metal Laminates Based on Jute and Glass Fabrics for Enhanced Mechanical Properties.” *Journal of Natural Fibers* 19 (1): 303–318. https://doi.org/10.1080/15440478.2020.1739594.

Abid, S. R., G. Murali, J. Ahmad, T. S. Al-Ghasham, and N. I. Vatin. 2022. “Repeated Drop-Weight Impact Testing of Fibrous Concrete: State-Of-The-Art Literature Review, Analysis of Results Variation and Test Improvement Suggestions.” *Materials* 15 (11): 15. https://doi.org/10.3390/ma15113948.

Aili Hamzah, A. F., M. H. Hamzah, H. Che Man, N. S. Jamali, S. I. Siajam, and M. H. Ismail. 2021. "Recent Updates on the Conversion of Pineapple Waste (Ananas Comosus) to Value-Added Products, Future Perspectives and Challenges." *Agronomy* 11 (11): 2221. https://doi.org/10.3390/agronomy11112221.

Allah, M. M. A., D. A. Hegazy, H. Alshahrani, T. A. Sebaey, and M. A. A. El-Baky. 2023. "Fiber Metal Laminates Based on Natural/Synthesis Fiber Composite for Vehicles Industry: An Experimental Comparative Study." *Fibers and Polymers* 24 (8): 2877–2889. https://doi.org/10.1007/s12221-023-00281-x.

Askarian Khoob, A., M. J. Ramezani, and S. S. Mousavi. 2023. "Low-Velocity Impact Resistance of Glass Laminate Aluminium Reinforced Epoxy (GLARE) Composite." *Recent Progress in Materials* 5 (02): 1–26. https://doi.org/10.21926/rpm.2302021.

Babu, T. N., S. Shyam, S. Kaul, and D. R. Prabha. 2021. "Natural Fibre Composites – an Alternative to Plastics in the Automotive Industry: A Review." *Proceedings of the Institution of Mechanical Engineers, Part L: Journal of Materials: Design and Applications* 236 (2): 237–266. https://doi.org/10.1177/14644207211041622.

Baigh, T. A., F. Nanzeeba, H. R. Hamim, and M. A. Habib. 2023. "A Comprehensive Study on the Effect of Hybridization and Stacking Sequence in Fabricating Cotton-Blended Jute and Pineapple Leaf Fibre Biocomposites." *Heliyon* 9 (9): e19792. https://doi.org/10.1016/j.heliyon.2023.e19792.

Barth, T., J. Wiedemann, T. Roloff, T. Behrens, N. Rauter, C. Hühne, M. Sinapius, et al. 2023. "Experimental Determination of Dispersion Diagrams Over Large Frequency Ranges for Guided Ultrasonic Waves in Fiber Metal Laminates." *Smart Materials & Structures* 32 (8): 085011. https://doi.org/10.1088/1361-665X/ace0ea.

Bornemann, S., and W. Lang. 2022. "Considerations and Limits of Embedding Sensor Nodes for Structural Health Monitoring into Fiber Metal Laminates." *Sensors (Switzerland)* 22 (12): 22. https://doi.org/10.3390/s22124511.

Chrispin Das, M., D. Arthur Jebastine Sunderraj, K. Arun Vasantha Geethan, D. Elilraja, T. Prabhuram, and S. Prathapsingh. 2022. "Mechanical and Moisture Absorption Behaviour of Woven Pineapple Leaf Phenol Formaldehyde Composites." *Materials Today: Proceedings* 62:1303–1307. https://doi.org/10.1016/j.matpr.2022.04.680.

Doddamani, S., S. M. Kulkarni, S. Joladarashi, M. K. T S, and A. K. Gurjar. 2023. "Analysis of Light Weight Natural Fiber Composites Against Ballistic Impact: A Review." *International Journal of Lightweight Materials and Manufacture* 6 (3): 450–468. https://doi.org/10.1016/j.ijlmm.2023.01.003.

Dua, S., H. Khatri, J. Naveen, M. Jawaid, K. Jayakrishna, M. N. F. Norrrahim, A. Rashedi, et al. 2023. "Potential of Natural Fiber Based Polymeric Composites for Cleaner Automotive Component Production -A Comprehensive Review." *Journal of Materials Research and Technology* 25:1086–1104. https://doi.org/10.1016/j.jmrt.2023.06.019.

Feng, N. L., S. D. Malingam, C. W. Ping, and M. Z. Selamat. 2022. "Mechanical Characterization of Metal-Composite Laminates Based on Cellulosic Kenaf and Pineapple Leaf Fiber." *Journal of Natural Fibers* 19 (6): 2163–2175. https://doi.org/10.1080/15440478.2020.1807437.

Fragoso-Medina, O., and F. Velázquez-Villegas. 2023. "Aluminum Foam to Improve Crash Safety Performance: A Numerical Simulation Approach for the Automotive Industry." *Mechanics Based Design of Structures and Machines* 51 (7): 3583–3597. https://doi.org/10.1080/15397734.2021.1927076.

Ganesarajan, D., L. Simon, S. Tamrakar, A. Kiziltas, D. Mielewski, N. Behabtu, C. Lenges, et al. 2022. "Hybrid Composites with Engineered Polysaccharides for Automotive Lightweight." *Composites Part C Open Access* 7:100222. https://doi.org/10.1016/j.jcomc.2021.100222.

Giammaria, V., S. Boria, F. Sarasini, J. Tirillò, F. Cognigni, M. Rossi, B. Fischer, et al. 2023. "Low-Velocity Impact Behaviour of Biocomposite Laminates Reinforced by Flax, Basalt and Hybrid Fibres at Various Temperatures: Analytical, Numerical and Experimental Results." *Composite Structures* 322:117332. https://doi.org/10.1016/j.compstruct.2023.117332.

Gupta, R. K., A. Mahato, and A. Bhattacharya. 2022. "Strength and Failure Behavior of Carbon Fiber Reinforced Aluminum Laminates Under Flexural Loading." *Mechanics of Advanced Materials and Structures* 29 (5): 662–676. https://doi.org/10.1080/15376494.2020.1786754.

Hashim, M. K. R., M. S. Abdul Majid, M. J. M. Ridzuan, F. H. Kasim, M. N. A. Uda, Z. A. Arsat, F. Abdullah, A. Firdaus, M. Muttalib, and M. N. Afnan Uda. 2023. "The Mechanical Properties of Pineapple Leaf Fibre (PALF)/Carbon Hybrid Laminate Composites at Anti-Symmetric Ply Orientation." *Materials Today: Proceedings*. https://doi.org/10.1016/j.matpr.2023.04.003.

Herlina Sari, N., S. Suteja, C. I. Pruncu, I. Setyawan, R. A. Ilyas, and L. Lamberti. 2024. "Physicomechanical, Water Absorption and Thermal Properties and Morphology of Paederia Foetida Fiber– Al 2 O 3 Powder Hybrid-Reinforced Epoxy Composites." *Polymer International* 73 (7): 573–585. https://doi.org/10.1002/pi.6632.

Hussain, M., A. Imad, Y. Nawab, A. Saouab, C. Herbelot, and T. Kanit. 2022. "Effect of Matrix and Hybrid Reinforcement on Fibre Metal Laminates Under Low–Velocity Impact Loading." *Composite Structures* 288:115371. https://doi.org/10.1016/j.compstruct.2022.115371.

Hynes, N. R. J., N. J. Vignesh, J. T. W. Jappes, P. S. Velu, C. Barile, M. A. Ali, M. U. Farooq, et al. 2022. "Effect of Stacking Sequence of Fibre Metal Laminates with Carbon Fibre Reinforced Composites on Mechanical Attributes: Numerical Simulations and Experimental Validation." *Composites Science and Technology* 221:109303. https://doi.org/10.1016/j.compscitech.2022.109303.

Ilyas, R. A., H. Aisyah, A. Nordin, N. Ngadi, M. Zuhri, M. Asyraf, S. Sapuan, et al. 2022. “Natural-Fiber-Reinforced Chitosan, Chitosan Blends and Their Nanocomposites for Various Advanced Applications.” *Polymers* 14 (5): 14. https://doi.org/10.3390/polym14050874.

Jain, J., S. Jain, and S. Sinha. 2018. “Characterization and Thermal Kinetic Analysis of Pineapple Leaf Fibers and Their Reinforcement in Epoxy.” *Journal of Elastomers & Plastics* 51 (3): 224–243. https://doi.org/10.1177/0095244318783024.

Kali, N., S. Pathak, and S. Korla. 2020. “Effect on Vibration Characteristics of Fiber Metal Laminates Sandwiched with Natural Fibers.” *Materials Today: Proceedings* 28:1092–1096. https://doi.org/10.1016/j.matpr.2020.01.088.

Khalid, M. Y., Z. U. Arif, A. Al Rashid, M. I. Shahid, W. Ahmed, A. F. Tariq, Z. Abbas, et al. 2021. “Interlaminar Shear Strength (ILSS) Characterization of Fiber Metal Laminates (FMLs) Manufactured Through VARTM Process.” *Forces in Mechanics* 4:100038. https://doi.org/10.1016/j.finmec.2021.100038.

Koh-Dzul, J. F., J. G. Carrillo, J. Guillen-Mallette, and E. A. Flores-Johnson. 2023. “Low Velocity Impact Behaviour and Mechanical Properties of Sandwich Panels with Cores Made from Tetra Pak Waste.” *Composite Structures* 304:116380. https://doi.org/10.1016/j.compstruct.2022.116380.

Kosedag, E., M. Aydin, and R. Ekici. 2022. “Effect of Stacking Sequence and Metal Volume Fraction on the Ballistic Impact Behaviors of ARALL Fiber-Metal Laminates: An Experimental Study.” *Polymer Composites* 43 (3): 1536–1545. https://doi.org/10.1002/pc.26474.

Lee, D.-W., B.-J. Park, S.-Y. Park, C.-H. Choi, and J.-I. Song. 2018. “Fabrication of High-Stiffness Fiber-Metal Laminates and Study of Their Behavior Under Low-Velocity Impact Loadings.” *Composite Structures* 189:61–69. https://doi.org/10.1016/j.compstruct.2018.01.044.

Liu, G., W. Gao, W. Liu, J. Xu, Y. Wei, T. Liu, L. Rui, et al. 2023. “Debonding Defect Detection by Applying Pulsed, Lock-In and Linear Frequency Modulation Thermal Excitation Methods in the Inspection of Fiber-Reinforced Metal Laminates.” *Russian Journal of Nondestructive Testing* 59 (8): 915–922. https://doi.org/10.1134/S106183092360051X.

Ma, Y., L. Wu, L. Yu, E. A. Elbadry, W. Yang, X. Huang, X. Yan, et al. 2021. “Effect of Fiber Breakage Position on the Mechanical Performance of Unidirectional Carbon Fiber/Epoxy Composites.” *Reviews on Advanced Materials Science* 60 (1): 352–364. https://doi.org/10.1515/rams-2021-0029.

Miao, W., Z. Xin, Y. Qin, Y. Wang, and H. Chen. 2022. “Dynamic Modeling of Particle Reinforced Composites and Its Charpy Impact Test Verification.” *Materials Today Communications* 30:103040. https://doi.org/10.1016/j.mtcomm.2021.103040.

Mohammadi, H., Z. Ahmad, S. A. Mazlan, M. A. Faizal Johari, G. Siebert, M. Petrů, S. S. Rahimian Koloor, et al. 2022. “Lightweight Glass Fiber-Reinforced Polymer Composite for Automotive Bumper Applications: A Review.” *Polymers* 15 (1): 15. https://doi.org/10.3390/polym15010193.

Muflikhun, M. A., and T. Yokozeki. 2021. “Steel Plate Cold Commercial - Carbon Fiber Reinforced Plastics Hybrid Laminates for Automotive Applications: Curing Perspective with Thermal Residual Effect.” *Journal of Materials Research and Technology* 14:2700–2714. https://doi.org/10.1016/j.jmrt.2021.07.152.

Murugu Nachippan, N., M. Alphonse, V. K. Bupesh Raja, S. Shasidhar, G. Varun Teja, and R. Harinath Reddy. 2021. “Experimental Investigation of Hemp Fiber Hybrid Composite Material for Automotive Application.” *Materials Today: Proceedings* 44:3666–3672. https://doi.org/10.1016/j.matpr.2020.10.798.

Najeeb, M. I., M. T. Hameed Sultan, A. U. Md Shah, S. M. Muhammad Amir, S. N. A. Safri, M. Jawaid, M. R. Shari, et al. 2021. “Low-Velocity Impact Analysis of Pineapple Leaf Fiber (PALF) Hybrid Composites.” *Polymers* 13 (18): 3194. https://doi.org/10.3390/polym13183194.

Naveen R., M. Kumar, C. Shwetha, and R. Rishekesh. 2020. *Sound Absorbing Performance of Hybrid Fiber Metal Laminate Composites, in ASCEND 2020*. Reston, VA: American Institute of Aeronautics and Astronautics.

Ng, L. F., M. Y. Yahya, C. Muthukumar, X. J. Woo, A. H. Muhaimin, and R. A. Majid. 2023. “Mechanical Characterization of Aluminum Sandwich Structures with Woven-Ply Pineapple Leaf/Glass Fiber-Reinforced Hybrid Composite Core.” *Journal of Natural Fibers* 20 (1): 2160404. https://doi.org/10.1080/15440478.2022.2160404.

Noorsumar, G., S. Rogovchenko, K. G. Robbersmyr, and D. Vysochinskiy. 2022. “Mathematical Models for Assessment of Vehicle Crashworthiness: A Review.” *International Journal of Crashworthiness* 27 (5): 1545–1559. https://doi.org/10.1080/13588265.2021.1929760.

Ortiz de Mendibil, I., L. Aretxabaleta, M. Sarrionandia, M. Mateos, and J. Aurrekoetxea. 2016. “Impact Behaviour of Glass Fibre-Reinforced Epoxy/Aluminium Fibre Metal Laminate Manufactured by Vacuum Assisted Resin Transfer Moulding.” *Composite Structures* 140:118–124. https://doi.org/10.1016/j.compstruct.2015.12.026.

Pang, Y., X. Yan, H. Yao, J. Qu, and L. Wu. 2022. “Experimental Study of Basalt Fiber/Steel Hybrid Laminates Under Low-Velocity Impact.” *Engineering Fracture Mechanics* 259:108169. https://doi.org/10.1016/j.engfracmech.2021.108169.

Ravi, Y. V., N. Kapilan, S. Rajole, Y. S. Balaji, N. Varun Kumar Reddy, and B. K. Venkatesha. 2022. “Damage Resistance Evaluation of E-Glass and Hybrid Hemp-Banana Natural Fiber Composite Helmet Using Drop Weight Impact Test.” *Materials Today: Proceedings* 54:330–335. https://doi.org/10.1016/j.matpr.2021.09.213.

Sari, N. H., S. Anu, S. M. Rangappa, and S. Siengchin. 2023. "A Review on Cellulose Fibers from Eichornia Crassipes: Synthesis, Modification, Properties and Their Composites." *Journal of Natural Fibers* 20 (1): 2162179. https://doi.org/10.1080/15440478.2022.2162179.

Shah, C., S. Bosse, C. Zinn, and A. von Hehl. 2023. "Optimization of Non-Destructive Damage Detection of Hidden Damages in Fiber Metal Laminates Using X-Ray Tomography and Machine Learning Algorithms." In *Advances in System-Integrated Intelligence*, edited by M. Valle, D. Lehmhus, C. Gianoglio, E. Ragusa, L. Seminara, S. Bosse, A. Ibrahim, and K.-D. Thoben, 387–402. Cham: Springer International Publishing.

Sharma, A. P., S. H. Khan, R. Kitey, and V. Parameswaran. 2018. "Effect of Through Thickness Metal Layer Distribution on the Low Velocity Impact Response of Fiber Metal Laminates." *Polymer Testing* 65:301–312. https://doi.org/10.1016/j.polymertesting.2017.12.001.

Siakeng, R., M. Jawaid, H. Ariffin, and S. M. Sapuan. 2019. "Mechanical, Dynamic, and Thermomechanical Properties of Coir/Pineapple Leaf Fiber Reinforced Polylactic Acid Hybrid Biocomposites." *Polymer Composites* 40 (5): 2000–2011. https://doi.org/10.1002/pc.24978.

Siddiqui, M. A. S., M. S. Rabbi, and S. Dewanjee. 2023. "Low-Velocity Impact Response of Natural Fiber Reinforced Composites: A Comprehensive Review on Influential Parameters." *Composites Part C Open Access* 12:100422. https://doi.org/10.1016/j.jcomc.2023.100422.

Stephen, C., A.-H. I. Mourad, B. Shivamurthy, and R. Selvam. 2021. "Energy Absorption and Damage Assessment of Non-Hybrid and Hybrid Fabric Epoxy Composite Laminates: Experimental and Numerical Study." *Journal of Materials Research and Technology* 14:3080–3091. https://doi.org/10.1016/j.jmrt.2021.08.108.

Syafri, E., J. Jamaluddin, N. H. Sari, M. Mahardika, L. Suryanegara, R. Sinaga, F. Yudhanto, et al. 2023. "Effect of Ultrafine Grinding and Ultrasonication Duration on the Performance of Polyvinyl Alcohol (PVA) Agave Gigantea Cellulose Micro Fiber (CMF) Bio-Composite Film." *Journal of Natural Fibers* 20 (1): 2192545. https://doi.org/10.1080/15440478.2023.2192545.

Vieira, L. M. G., Y. Dobah, J. C. dos Santos, T. H. Panzera, J. C. Campos Rubio, and F. Scarpa. 2022. "Impact Properties of Novel Natural Fibre Metal Laminated Composite Materials." *Applied Sciences* 12 (4): 12. https://doi.org/10.3390/app12041869.

Wu, X., L. Zhan, X. Zhao, X. Wang, and T. Chang. 2020. "Effects of Surface Pre-Treatment and Adhesive Quantity on Interface Characteristics of Fiber Metal Laminates." *Composite Interfaces* 27 (9): 829–843. https://doi.org/10.1080/09276440.2019.1707023.

Xiao, H., M. T. H. Sultan, F. S. Shahar, M. Gaff, and D. Hui. 2023. "Recent Developments in the Mechanical Properties of Hybrid Fiber Metal Laminates in the Automotive Industry: A Review." *Reviews on Advanced Materials Science* 62 (1): 62. https://doi.org/10.1515/rams-2022-0328.

Xiao, H., M. T. H. Sultan, F. S. Shahar, and S. Y. Nayak. 2024. "Mechanical and Viscoelastic Behavior Characterization of Hybrid Aluminum/Carbon Fiber/Pineapple Leaf Fiber Composite via VARTM for Automotive Industry." *Journal of Natural Fibers* 21 (1): 2382874. https://doi.org/10.1080/15440478.2024.2382874.

Xiao, H., M. T. H. Sultan, F. S. Shahar, S. Y. Nayak, N. Yidris, and A. U. M. Shah. 2023. "Development of Hybrid Aluminum/Carbon Fiber/Pineapple Leaf Fiber Laminates Using Vacuum Assisted Resin Transfer Molding (VARTM) for Automotive Applications." *Applied Composite Materials* 31 (2): 561–581. https://doi.org/10.1007/s10443-023-10183-z.

Xie, J., C. Xu, C. Wu, L. Gao, G. Chen, G. Li, G. Song, et al. 2023. "Visualization of Defects in CFRP-Reinforced Steel Structures Using Improved Eddy Current Pulsed Thermography." *Automation in Construction* 145:104643. https://doi.org/10.1016/j.autcon.2022.104643.

Yanyan, L., H. Li, Q. Wang, Z. Gong, and J. Tao. 2020. "Effect of Plasma Surface Treatment of Aluminum Alloy Sheet on the Properties of Al/Gf/PP Laminates." *Applied Surface Science* 507:145062. https://doi.org/10.1016/j.apsusc.2019.145062.

Zhang, F., Y. Lin, J. A. Wu, Z. Zhang, Y. Huang, C. Li, M. Wang, et al. 2022. "Comparison of Stacking Sequence on the Low-Velocity Impact Failure Mechanisms and Energy Dissipation Characteristics of CFRP/Al Hybrid Laminates." *Polymer Composites* 43 (8): 5544–5562. https://doi.org/10.1002/pc.26867.

Zhang, J., Y. Wang, Y. Wen, X. Dai, Y. Zhao, and G. Fang. 2023. "Energy Dissipation Mechanism of Fiber Metal Laminate Under Low-Velocity Impact." *Thin-Walled Structures* 183:110355. https://doi.org/10.1016/j.tws.2022.110355.

Zhang, W., and J. Xu. 2022. "Advanced Lightweight Materials for Automobiles: A Review." *Materials & Design* 221:110994. https://doi.org/10.1016/j.matdes.2022.110994.

Zhu, J., Z. Mao, D. Wu, J. Zhou, D. Jiao, W. Shi, W. Zhu, et al. 2022. "Progress and Trends in Non-Destructive Testing for Thermal Barrier Coatings Based on Infrared Thermography: A Review." *Journal of Nondestructive Evaluation* 41 (3): 49. https://doi.org/10.1007/s10921-022-00880-3.

Zhu, W., H. Xiao, J. Wang, and C. Fu. 2019. "Characterization and Properties of AA6061-Based Fiber Metal Laminates with Different Aluminum-Surface Pretreatments." *Composite Structures* 227:111321. https://doi.org/10.1016/j.compstruct.2019.111321.